# On computing sound radiation of a temporally evolving mixing layer by vortex method and matched asymptotic expansions

F. Q. Hu<sup>(1)</sup>, J. E. Martin<sup>(2)</sup>, M. Y. Hussaini<sup>(3)</sup>

(1) Department of Mathematics and Statistics, Old Dominion University Norfolk, VA 23529

(2)Department of Mathematics, Christopher Newport University Newport News, VA 23606

(3)Institute for Computer Applications in Science and Engineering NASA Langley Research Center, Hampton, VA 23681

# ABSTRACT

In this paper, sound radiation associated with a temporally evolving mixing layer is considered. Numerical simulations are carried out by a vortex method in which the mixing layer is modeled by an array of vortex blobs and perturbed with the wavelength of the most amplified wave. Since the vortex method computes an incompressible flow, a methodology of computing the acoustic field based on matched asymptotic expansions is employed. A singular perturbation is developed in which the incompressible solution obtained by the vortex method is the inner solution while the acoustic field is the outer solution. The formal matching process is carried out by introducing intermediate variables. It is shown that in the limit of zero Mach number, the leading terms match smoothly. The inner solution of the incompressible flow thus provides the boundary condition for the outer solution of radiated sound. Numerical results of the vortex simulation and computed acoustic pressure are presented.

#### I. INTRODUCTION

Vortex methods have many attractive advantages in numerical simulation of flows of practical interest, such as mixing layers and jets. They are also of interest to computational aeroacoustics in connection with the vortex sound theory of low Mach number

Copyright c 1996 by the American Institute of Aeronautics and Astronautics, Inc. All rights reserved.

flows. Powell<sup>15</sup> first proposed the concept of vortex sound in which the source term in Lighthill's acoustic analogy<sup>10</sup> is related to the vorticity of the flow at low Mach numbers. Later, using a method of matched asymptotic expansions,  $\operatorname{Crow}^4$  showed that the source term in the acoustic analogy can be computed using incompressible flow variables when the source is compact. The sound source is considered compact if  $\ell/\lambda << 1$  where  $\ell$  is the turbulent eddy size and  $\lambda$  is the acoustic length scale. The method of matched asymptotic expansions has also been used in many other problems of sound radiation, including that of two co-rotating vortices<sup>3,8,14</sup>.

Since the vorticity field is intimately related to the sound source in the vortex sound theory, several studies have emerged recently in which numerical simulations based on vortex methods are used to compute the sound radiation. In [7], the acoustic field associated with the regular and chaotic motions of three point vortices is computed based on a Powell-Hardin formulation of the vortex sound theory. In that work, the motion of three vortices is simulated using a vortex method and the acoustic pressure is found by evaluating the source term numerically. In [6], the acoustic field associated with the collision of two vortex rings is computed numerically.

The present work explores the viability of vortex methods for computing sound radiation of low Mach number flows based on matched asymptotic expansions. In particular, the induced sound field of a two-dimensional temporally evolving planar mixing layer is considered. Simulations of the mixing layer are conducted by a vortex method in which the mixing layer is modeled by an array of vortex blobs and perturbed with the wavelength of the most

<sup>(1)</sup> Assistant Professor, Member AIAA

<sup>(2)</sup> Assistant Professor

<sup>(3)</sup>Director, Associate Fellow AIAA

amplified wave. The mixing layer is assumed to be periodic in the direction of the mean flow. initial exponential growth as well as the non-linear growth of the mixing layer are computed. However, the present vortex method, as well as most vortex methods currently in use, computes an incompressible flow. Furthermore, since the mixing layer has an infinite extent, the sound source is non-compact. To compute the radiated sound field associated with the temporal evolution of the mixing layer, a methodology of matched asymptotic expansions is employed. A detailed analysis of matched asymptotic expansions for the temporally evolving mixing layer is presented. The far-field acoustic problem will be treated as a singular perturbation problem in the limit of zero Mach number. For the flow field close to the mixing layer, the characteristic velocity and length scales are the mean velocity and the vorticity wavelength. The near field flow is incompressible to leading order in a small Mach number expansion. At the far field, the proper velocity and length scales are the speed of sound and the acoustic wavelength. There, the linearized equation for the acoustic waves is the convected wave equation. A singular perturbation is developed using the method of matched asymptotic expansions. In this approach, the incompressible solution obtained by the vortex method is the inner solution while the acoustic field is the outer solution. The formal matching process is carried out by introducing intermediate variables. It is shown that in the limit of zero Mach number, the leading terms match smoothly. The inner solution of the incompressible flow thus provides the boundary conditions for the outer solution of radiated sound.

In the next section, formulations of the vortex method and matched asymptotic expansions are given. Numerical results are presented in section 3. Section 4 contains the conclusions.

#### II. FORMULATION

We consider the temporal evolution of a planar mixing layer, modeled by an array of vortex blobs. The mean velocities are  $U_{\infty}$  and  $-U_{\infty}$  for the fluids above and below the mixing layer, respectively.

In the next two sub-sections, formulations of the vortex method for simulating the mixing layer and the method of matched asymptotic expansion for computing the far-field acoustic waves are given.

# A. Vortex Method

Since the generation, growth and merging of the

large scale mixing layer vortices is dominated by inviscid mechanisms, we employ a two-dimensional vortex dynamics technique for the simulation of Euler's equations. These methods, as reviewed by Leonard9. are well established and offer an efficient and conceptually straightforward way to capture the large scale features of evolving free shear flows. A brief description of the particular variant employed in this study is given in the following. The rotational portion of the fluid is discretized into a row of N vortex blobs of radius  $\sigma$  and circulation  $\Gamma_i$  (i=1,N). The basic assumption that the flow field is inviscid then allows one to make use of the theorems of Kelvin and Helmholtz to advance the blobs as material elements according to the Biot-Savart law2, while maintaining their circulation  $\Gamma_i$  as being fixed. We consider the case of a streamwise periodic, temporally evolving mixing layer. This model captures all of the dominant features of a mixing layer, including the instability of the vorticity layer, the formation and subsequent pairing of the large scale spanwise vortices and the inherent strain field. Furthermore, the temporally evolving case is numerically more efficient and it avoids the problem of assigning inflow and outflow boundary conditions. We obtain a smooth vorticity field by employing an invariant vorticity distribution of the form

$$\omega(r) = \Gamma_i / (\pi \sigma^2) \exp(-r^2 / \sigma^2) \tag{1}$$

in which r is the radial distance from the blob center. For the calculation of the velocity field, the Biot-Savart law requires integration over the entire vorticity field. Therefore, the far field effect of the streamwise periodic images of the blobs must also be taken into account. This can be evaluated analytically by treating the images of the vortex blobs as point vortices, so that the overall velocities in the streamwise and cross-stream directions respectively, are given by

$$u(x,y) = \sum_{i=1}^{N} \left\{ \frac{1}{2\pi} \frac{y - y_i}{r^2} \Gamma_i \exp(-r^2/\sigma^2) - \frac{\Gamma_i}{2L} \frac{\sinh[2\pi(y - y_i)/L]}{\cosh[2\pi(y - y_i)/L] - \cos[2\pi(x - x_i)/L]} \right\}$$

$$v(x,y) = \sum_{i=1}^{N} \left\{ -\frac{1}{2\pi} \frac{x - x_i}{r^2} \Gamma_i \exp(-r^2/\sigma^2) + \frac{\Gamma_i}{2L} \frac{\sin[2\pi(x - x_i)/L]}{\cosh[2\pi(y - y_i)/L] - \cos[2\pi(x - x_i)/L]} \right\}$$
(2b)

in which  $(x_i, y_i)$  represents the time dependent position of each blob and L is the streamwise dimension of the periodic control volume. We advance the flow field in time by calculating the velocity induced at the center of each blob  $\mathbf{u}(\mathbf{x}_j,t)$  and by advancing the blobs' positions  $\mathbf{x}_j$  according to the equation.

$$\frac{d\mathbf{x}_j}{dt} = \mathbf{u}(\mathbf{x}_j, t) \tag{3}$$

where summation in equation (1) now takes place for all i not equal to j. A second order accurate predictor-corrector scheme is used for the time integration of the blob positions. To determine the optimal spatial discretization, the number of blobs was increased until no further change in the maximum vorticity occurred during the evolution of the flow. Typically, this resulted in a discretization of 59 blobs per basic wavelength.

In analogy to forcing the flow in an experiment, we initially impose a sinusoidal modification to the strength of the vortex blobs<sup>13</sup>. This perturbation induces the instability and roll up of the shear layer. It is given by

$$\Gamma_i = \Gamma_{io}(1 + .05 \sin \alpha x)$$

where  $\Gamma_{io}$  is the vortex blob strength corresponding to the unperturbed flow. The wavenumber  $\alpha$  of the perturbation is chosen to be approximately the maximally amplified wavenumber as predicted by the inviscid stability analysis of Michalke<sup>11</sup>.

# B. Matched Asymptotic Expansions

#### B.1 Governing equations of a compressible flow

To study the acoustic field associated with the temporal evolution of the mixing layer, we consider the governing equations for the inviscid compressible flow which include

continuity equation:

$$\frac{\partial \rho}{\partial t} + \frac{\partial \rho u}{\partial x} + \frac{\partial \rho v}{\partial y} = 0 \tag{4a}$$

momentum equation:

$$\frac{\partial u}{\partial t} + u \frac{\partial u}{\partial x} + v \frac{\partial u}{\partial y} = -\frac{1}{\rho} \frac{\partial p}{\partial x}$$
 (4b)

$$\frac{\partial v}{\partial t} + u \frac{\partial v}{\partial x} + v \frac{\partial v}{\partial y} = -\frac{1}{\rho} \frac{\partial p}{\partial y} \tag{4c}$$

and the isentropic relation

$$p = \kappa \rho^{\gamma} \tag{4d}$$

where u and v are the velocities in the x and y directions respectively, p is the pressure,  $\rho$  is the density and  $\gamma$  is the ratio of specific heats. The speed of sound is  $a = (\gamma p/\rho)^{\frac{1}{2}}$ .

We assume that the vorticities are confined inside a layer of thickness 2d such that the flow is irrotational for |y| > d. Outside this layer, we can introduce a potential function  $\phi$  for the velocity field, i.e..

$$u = \frac{\partial \phi}{\partial x}, \quad v = \frac{\partial \phi}{\partial y} \tag{5}$$

By substituting (5) into (4), an equation for  $\phi$  can be found<sup>5,12</sup>:

$$\frac{\partial^2 \phi}{\partial t^2} - a_{\infty}^2 \nabla^2 \phi = -\frac{\partial \Phi}{\partial t} - \frac{1}{2} \frac{\partial \phi}{\partial x} \frac{\partial \Phi}{\partial x} - \frac{1}{2} \frac{\partial \phi}{\partial y} \frac{\partial \Phi}{\partial y} + (a^2 - a_{\infty}^2) \nabla^2 \phi$$
(6)

in which

$$\Phi = \left(\frac{\partial \phi}{\partial x}\right)^2 + \left(\frac{\partial \phi}{\partial y}\right)^2$$
 and  $\nabla^2 \phi = \frac{\partial^2 \phi}{\partial x^2} + \frac{\partial^2 \phi}{\partial y^2}$ 

and  $a_{\infty}$  is the mean speed of sound in the far field. Moreover, upon integrating the momentum equations, we get

$$\frac{\partial \phi}{\partial t} + \frac{1}{2} \left[ \left( \frac{\partial \phi}{\partial x} \right)^2 + \left( \frac{\partial \phi}{\partial y} \right)^2 \right] + \int \frac{dp}{\rho} = C(t)$$

where C(t) is a function of time. By letting  $y \to \infty$  and utilizing (4), we further get

$$\frac{\partial \phi}{\partial t} + \frac{1}{2} \left[ \left( \frac{\partial \phi}{\partial x} \right)^2 + \left( \frac{\partial \phi}{\partial y} \right)^2 \right] + \frac{\gamma}{\gamma - 1} \frac{p}{\rho} = \frac{1}{2} U_{\infty}^2 + \frac{\gamma}{\gamma - 1} \frac{p_{\infty}}{\rho_{\infty}}$$
(7a)

where  $p_{\infty}$  and  $\rho_{\infty}$  are the reference pressure and density of the far field. On the other hand, for incompressible flows, where  $\rho$  is constant, we have

$$\frac{\partial \phi}{\partial t} + \frac{1}{2} \left[ \left( \frac{\partial \phi}{\partial x} \right)^2 + \left( \frac{\partial \phi}{\partial y} \right)^2 \right] + \frac{p}{\rho_{\infty}} = \frac{1}{2} U_{\infty}^2 + \frac{p_{\infty}}{\rho_{\infty}}$$
(7b)

### **B.2** Inner solution

For simplicity, we will consider the flow field above the mixing layer, i.e., the upper half-plane. The lower half-plane can be treated analogously. Close to the mixing layer, the characteristic velocity and length scales are the mean velocity  $U_{\infty}$  and wavelength L of the instability wave. Let the scaled inner variables be

$$x^{i} = \frac{2\pi x}{L}, \quad y^{i} = \frac{2\pi y}{L}, \quad t^{i} = \frac{2\pi t}{L/U_{\infty}}$$
$$u^{i} = \frac{u}{U_{\infty}}, \quad v^{i} = \frac{v}{U_{\infty}}, \quad \phi^{i} = \frac{2\pi \phi}{U_{\infty}L}$$
$$p^{i} = \frac{p - p_{\infty}}{\rho_{\infty}U_{\infty}^{2}}, \quad \rho^{i} = \frac{\rho - \rho_{\infty}}{\rho_{\infty}}$$

where a superscript i has been used to indicate the inner variables. For convenience, the non-dimensionalized wavelength is taken to be  $2\pi$ . Then, equation (6) becomes

$$M^{2} \frac{\partial^{2} \phi^{i}}{\partial t^{i^{2}}} - \nabla^{i^{2}} \phi^{i} = -M^{2} \frac{\partial \Phi^{i}}{\partial t^{i}} - \frac{1}{2} M^{2} \left[ \frac{\partial \phi^{i}}{\partial x^{i}} \frac{\partial \Phi^{i}}{\partial x^{i}} + \frac{\partial \phi^{i}}{\partial y^{i}} \frac{\partial \Phi^{i}}{\partial y^{i}} \right] + \frac{a^{2} - a_{\infty}^{2}}{a_{\infty}^{2}} \nabla^{i^{2}} \phi^{i}$$
(8)

where  $M = U_{\infty}/a_{\infty}$  is the Mach number and is assumed to be a small parameter. It can also be shown that the coefficient of the last term in (8) is of order  $M^2$ .

We now express  $\phi^i$  as a power series in  $M^2$  as follows.

$$\phi^{i} = x^{i} + \phi^{i}_{0} + M^{2}\phi^{i}_{1} + \cdots$$
 (9)

where the first term represents the mean flow. From (8), it follows that, for the leading term,

$$\nabla^{i^2} \phi^{i}_{0} = 0 \tag{10}$$

Thus, to the leading order, the flow field near the mixing layer is the same as that of the incompressible flow, which can be computed using the vortex method. Upon a linearization of equation (7b), it is found that the leading order pressure,  $p^i_0$ , is related to the potential  $\phi^i_0$  as

$$p^{i}_{0} = -\left(\frac{\partial \phi^{i}_{0}}{\partial t^{i}} + \frac{\partial \phi^{i}_{0}}{\partial x^{i}}\right) \tag{11}$$

for  $y^i$  large. Moreover,  $p^i_{\ 0}$  also satisfies the Laplace equation

$$\nabla^{i^2} \, p^i_{\ 0} = 0 \tag{12}$$

The asymptotic form of  $p^{i}_{0}$  for  $y^{i}$  large will be considered next. Since the vortex simulation is

periodic in  $x^i$ , we express the inner solution for the pressure as a Fourier series in  $x^i$  as

$$p^{i}_{0}(x^{i}, y^{i}, t^{i}) = \sum_{k=-\infty}^{\infty} \hat{p^{i}}_{k}(y^{i}, t^{i})e^{ikx'}$$
 (13)

By substituting the above into (12), it follows that, for  $y^i$  large,

$$\hat{p}^{i}_{k}(y^{i}, t^{i}) = \tilde{p}^{i}_{k}(t^{i})e^{-|k|y^{i}}$$

Thus, the asymptotic form of the inner solution, for the leading term, as  $y^i \to \infty$  is

$$p^{i}_{0}(x^{i}, y^{i}, t^{i}) = \sum_{k=-\infty}^{\infty} \tilde{p}^{i}_{k}(t^{i})e^{-|k|y^{i}}e^{ikx^{i}}$$
 (14)

### B.3 Outer solution

In the far field, the characteristic velocity and length scales are the sound speed  $a_{\infty}$  and wavelength  $\lambda$ . We define the following outer variables:

$$x^o = \frac{2\pi x}{\lambda}, \quad y^o = \frac{2\pi y}{\lambda}, \quad t^o = \frac{2\pi t}{\lambda/a_\infty}$$
 $u^o = \frac{u}{a_\infty}, \quad v^o = \frac{v}{a_\infty}, \quad \phi^o = \frac{2\pi \phi}{a_\infty \lambda}$ 
 $p^o = \frac{p - p_\infty}{\rho_\infty a_\infty^2}, \quad \rho^o = \frac{\rho - \rho_\infty}{\rho_\infty}$ 

where a superscript o has been used to denote the outer variables. The length scale for the acoustic waves is chosen as

$$\lambda = a_{\infty} \frac{L}{U_{\infty}} = \frac{L}{M} \tag{15}$$

Consequently, the scaled time for inner and outer solutions is the same, i.e.,  $t^i = t^o$ . In outer variables, equation (6) for the velocity potential becomes

$$\frac{\partial^{2} \phi^{\circ}}{\partial \hat{t}^{2}} - \nabla^{\circ 2} \phi^{\circ} = -\frac{\partial \Phi^{\circ}}{\partial t^{\circ}} - \frac{1}{2} \left[ \frac{\partial \phi^{\circ}}{\partial x^{\circ}} \frac{\partial \Phi^{\circ}}{\partial x^{\circ}} + \frac{\partial \phi^{\circ}}{\partial y^{\circ}} \frac{\partial \Phi^{\circ}}{\partial y^{\circ}} \right] + \frac{a^{2} - a_{\infty}^{2}}{a_{\infty}^{2}} \nabla^{\circ 2} \phi^{\circ} \tag{16}$$

Again, we express  $\phi^o$  as a power series of  $M^2$  as follows,

$$\phi^{o} = Mx^{o} + \phi^{o}_{0} + M^{2}\phi^{o}_{1} + \cdots$$
 (17)

where the first term represents the mean flow. By substituting (17) into (16), we get the equation for the leading term  $\phi_0^{\circ}$ 

$$\left(\frac{\partial}{\partial t^o} + M \frac{\partial}{\partial x^o}\right)^2 \phi^o_0 - \nabla^{o^2} \phi^o_0 = 0 \qquad (18)$$

The leading acoustic pressure disturbances,  $p^o_0$ , can also be found from the potential function by linearizing equation (7a) as

$$p^{o}_{0} = -\left(\frac{\partial \phi^{o}_{0}}{\partial t^{o}} + M \frac{\partial \phi^{o}_{0}}{\partial x^{o}}\right) \tag{19}$$

Moreover,  $p^{o}_{0}$  also satisfies the convective wave equation

$$\left(\frac{\partial}{\partial t^o} + M \frac{\partial}{\partial x^o}\right)^2 p^o_0 - \nabla^{o2} p^o_0 = 0 \qquad (20)$$

To facilitate the matching of the inner and outer solutions, we apply the following Fourier expansion to the outer solution

$$p^{o}_{0}(x^{o}, y^{o}, t^{o}) = \sum_{k=-\infty}^{\infty} p^{o}_{k}(y^{o}, t^{o}) e^{ik/M(x^{o} - Mt^{o})}$$
(21)

By substituting (21) into (20), it is easy to see that the amplitudes of the expansion,  $p_k^o(y^o, t^o)$ , satisfy the equation

$$\frac{\partial^2 \hat{p^o}_k}{\partial t^{o^2}} - \frac{\partial^2 \hat{p^o}_k}{\partial u^{o^2}} + \hat{k}^2 \hat{p^o}_k = 0 \tag{22}$$

where k = k/M. This is the Klein-Gordon equation. The solution to equation (22) is uniquely determined with the following boundary conditions<sup>16</sup>:

at 
$$y^o = 0$$
,  $p_k^o(0, t^o) = f_k(t^o)$  (23)

at  $y^o \rightarrow \infty$ ,  $p^o_k(0, t^o)$  satisfies the radiation condition (24)

and initial conditions:

at 
$$t^{\circ} = 0$$
,  $\hat{p^{\circ}}_{k}(y^{\circ}, 0) = \frac{\partial \hat{p^{\circ}}_{k}}{\partial t^{\circ}}(y^{\circ}, 0) = 0$  (25)

in which  $f_k(t^o)$  is to be determined in the matching process.

The above initial-boundary value problem can be solved using Laplace transforms<sup>16</sup>. It is found that, in terms of the boundary condition  $f_k(t^o)$ ,

$$\hat{p^{o}}_{k}(y^{o}, t^{o}) = f_{k}(t^{o} - y^{o}) - \int_{0}^{t^{o} - y^{o}} f_{k}(\tau) \frac{\hat{k}y^{o}}{\sqrt{(\tau - t^{o})^{2} - y^{o}^{2}}} \times J_{1}(\hat{k}\sqrt{(\tau - t^{o})^{2} - y^{o}^{2}}) d\tau \tag{26}$$

where  $J_1$  is the Bessel function of order unity. By means of Laplace Transform (see Appendix), the above can also be expressed as

$$p^{\circ}_{k}(t^{\circ}, y^{\circ}) = \frac{1}{2\pi} \int_{C} \tilde{f}_{k}(\omega) e^{-y^{\circ}\sqrt{\hat{k}^{2} - \omega^{2}}} d\omega \qquad (26')$$

where  $\tilde{f}_k(\omega)$  is the Laplace Transform of  $f_k(t^o)$ .

# B.4 Matching of inner and outer solutions

To show that the inner and outer solutions match as  $M \to 0$ , we introduce the intermediate variables  $\xi$  and  $\eta$  such that

$$x^i = M^{\alpha-1}\xi, \quad y^i = M^{\alpha-1}\eta$$

and

$$x^o = M^\alpha \xi, \quad y^o = M^\alpha \eta$$

where  $\alpha$  is some positive number and  $0 < \alpha < 1$ . We consider the intermediate limit  $M \to 0$  with  $\xi$  and  $\eta$  fixed. The matching will be carried out by expressing the inner and outer solutions in terms of the intermediate variables.

In the limit  $M \to 0$ , the inner variables  $x^i, y^i \to \infty$ . Thus, the inner solution, by (14), has the form of

$$p^{i}_{0} = \sum_{k=-\infty}^{\infty} \tilde{p^{i}}_{k}(t^{i}) e^{-|k|M^{\alpha-1}\eta} e^{ikM^{\alpha-1}\xi}$$
 (27)

The outer solution of (21), on the other hand, can be expressed as

$$p^{\circ}_{0} = \sum_{k=-\infty}^{\infty} \hat{p^{\circ}}_{k}(y^{\circ}, t^{\circ}) e^{ikM^{\alpha-1}\xi - ikt^{\circ}}$$
 (28)

By introducing Laplace Transforms (see Appendix), the leading term of  $p^o_k(y^o, t^o)$ , in the limit  $M \to 0$  is found to be

$$\hat{p^o}_k(y^o, t^o) \approx f_k(t^o) e^{-|k|M^{\alpha-1}\eta}$$
 (29)

Thus, (28) is of the form

$$p^{\circ}_{0} = \sum_{k=-\infty}^{\infty} f_{k}(t^{\circ}) e^{-|k|M^{\alpha-1}\eta} e^{ikM^{\alpha-1}\xi - ikt^{\circ}}$$
 (30)

Upon comparing (27) and (30), it is seen that the outer and inner solutions will match smoothly when

$$f_k(t^o) = M^2 \tilde{p_k}(t^i) e^{ikt^o}$$
 (31)

Thus, the boundary condition of the outer problem is related to the inner solution by (31).

#### III. NUMERICAL RESULTS

In this section, numerical results of the vortex simulation and the acoustic pressure computed by (26) will be presented. The simulation of the Kelvin-Helmholtz instability wave is shown in Figure 2, where the contour plots of vorticity are given for selected time steps. In Figure 3, the evolution of the vortex blobs and the contours of the induced incompressible pressure field are shown for selected time steps. The incompressible pressure is computed using (11) in which the potential is obtained as the summation of all the potential functions corresponding to the blobs. Then, a Fourier transform is performed in the x direction on the pressure field to extract the amplitudes  $p_k^i(y^i, t^i)$ , as in (13). The amplitude as a function of time at  $y^i = 5$  is shown in Figure 4 for k = 1 to 5. We note that k = 1 is the wavenumber of the fundamental mode, i.e., the forcing wave. It is seen that the fundamental mode grows exponentially as a function of time with a growth rate of 0.3947. On the other hand, the amplitudes  $p_k^i(y^i, t^i)$  decay exponentially as functions of  $y^i$  outside the mixing region, as shown in Figure 5.

The associated acoustic pressure at the far-field is computed by (26), in which the function  $f_k(t^o)$ is obtained by (31), i.e., the results of the vortex simulation. Here, we discuss some numerical considerations in evaluating the expressions in (26). First, the numerical evaluation of the integral in (26) requires a high order of accuracy since the value of the acoustic pressure is several orders of magnitude smaller than that of the individual terms in (26). An 8th-order numerical quadrature is used to compute the integral. The numerical results are also verified with refined integration intervals. Second, for the initial-boundary conditions given in (23)-(25) to be consistent, it is required that  $f_k(0) = 0$ . However, this is not satisfied by (31) since the vortex simulation is started with a non-zero initial perturbation. Our numerical computations have shown that when the results of the vortex simulation,  $p_k^i(t^i)$  as shown in Figure 3, were used directly, large acoustic pressure was resulted near  $t^o = y^o$  as an artifact of  $p_k^i(0) \neq 0$ . We thus modify the initial time in the integration to be  $t^o = -T_0$  such that  $p^i_k(-T_0)$  is less than  $10^{-20}$ . The values of  $p^i_{k}(t^i)$  for  $t^i < 0$  are obtained by extrapolation, assuming an exponential decay as  $t^i - -\infty$ .

In Figure 6, the associated acoustic pressures are shown as a function of time  $t^o$  at  $y^o = 20$  for the first mode, i.e., for k = 1. The Mach numbers are 0.08 and 0.16 respectively. The spectrum of  $\hat{p^o}_k(y^o, t^o)$  is shown in Figure 7 for several Mach numbers. As the Mach number increases, the amplitude increases and the spectrum shifts to the left. We also note that, for a given Mach number M, the peak of the spectrum is found for  $\omega > k/M$  (here k = 1 for the first mode) as indicated in dashed lines. That is, considering the expression (21), the radiated sound waves have supersonic phase speed relative to the mean flow.

Numerical results of  $p^{\sigma}_{k}(y^{\sigma}, t^{\sigma})$  for the second mode, k=2, are also shown in Figure 8 and 9 for M=0.2. In general, we found that the sound pressure induced by the second mode is significantly smaller than that of the fundamental mode. Again, the spectrum indicates that the radiated sound wave has supersonic phase speed relative to the mean flow.

#### IV. CONCLUSIONS

A singular perturbation is developed in which the incompressible solution obtained by the vortex method is the inner solution and the acoustic field is the outer solution. It is shown that in the limit of zero Mach number, the leading terms match smoothly. The inner solution of the incompressible flow thus provides the boundary condition for the outer solution of radiated sound. Numerical results indicate that the amplitude of the radiated acoustic waves increases with the Mach number. The spectrum also shows that the radiated waves have supersonic phase speed relative to the mean flow.

#### APPENDIX

In this appendix, we give the estimate of the outer solution  $\hat{p^o}_k(y^o, t^o)$  as  $M \to 0$ . For convenience, let

$$S(y^{o}, t^{o}) = \frac{\hat{k} y^{o}}{\sqrt{t^{o^{2}} - y^{o^{2}}}} J_{1}(\hat{k} \sqrt{t^{o^{2}} - y^{o^{2}}}) H(t^{o} - y^{o})$$
(A1)

where  $H(t^o - y^o)$  is a step function which equals to unity for positive arguments and zero otherwise. By utilizing the convolution theorem of the Laplace Transform, (26) can be written as

$$\begin{split} p^{\circ}_{k}(t^{\circ}, y^{\circ}) &= f_{k}(t^{\circ} - y^{\circ}) - \int_{0}^{t^{\circ}} f_{k}(\tau) S(y^{\circ}, t^{\circ} - \tau) d\tau \\ &= f_{k}(t^{\circ} - y^{\circ}) - \frac{1}{2\pi} \int_{C} \tilde{f}_{k}(\omega) \tilde{S}(y^{\circ}, \omega) e^{-i\omega t^{\circ}} d\omega \end{split}$$

where  $\tilde{f}_k(\omega)$  and  $\tilde{S}(y^o, \omega)$  are the Laplace transforms of  $f_k(t^o)$  and  $S(y^o, t^o)$ , and the inversion contour C is above all the poles of  $\tilde{f}_k$  and  $\tilde{S}$ . Furthermore, we note that the Laplace Transform of  $S(y^o, t^o)$  is 1

$$\tilde{S}(y^{o}, \omega) = \epsilon^{i\omega y^{o}} - e^{-y^{o}\sqrt{\tilde{k}^{2} - \omega^{2}}}$$
 (A2)

Thus,  $p_{k}^{o}(t^{o}, y^{o})$  can be expressed as

$$p^{o}_{k}(t^{o}, y^{o}) = f_{k}(t^{o} - y^{o})$$

$$- \frac{1}{2\pi} \int_{C} \tilde{f}_{k}(\omega) \left[ e^{i\omega y^{o}} - e^{-y^{o}\sqrt{\hat{k}^{2} - \omega^{2}}} \right] e^{-i\omega t^{o}} d\omega$$

$$= \frac{1}{2\pi} \int_{C} \tilde{f}_{k}(\omega) e^{-y^{o}\sqrt{\hat{k}^{2} - \omega^{2}}} d\omega \qquad (A3)$$

For the asymptotic form of  $p_k^{\alpha}(t^{\alpha}, y^{\alpha})$  as  $M \to 0$ , we substitute  $y^{\alpha} = M^{\alpha}\eta$  and k = k/M into (A3) and obtain

$$p^{\alpha}_{k}(t^{\alpha}, y^{\alpha}) = \frac{1}{2\pi} \int_{C} \tilde{f}_{k}(\omega) e^{-M^{\alpha} \eta \sqrt{(k/M)^{2} - \omega^{2}}} e^{-i\omega t^{\alpha}} d\omega$$
(A4)

Here the branch cuts of  $\sqrt{(k/M)^2 - \omega^2}$  will be specified such that

$$\operatorname{real}(\sqrt{(k/M)^2 - \omega^2}) > 0$$

To estimate expression (A4), we deform the contour C to be slightly above the real axis of the  $\omega$ -plane and express the integral as

$$p^{\sigma}_{k}(t^{\sigma}, y^{\sigma}) = \left( \int_{-\infty + i\epsilon}^{-|k|/M + \delta + i\epsilon} + \int_{-|k|/M + \delta + i\epsilon}^{|k|/M - \delta + i\epsilon} + \int_{|k|/M - \delta + i\epsilon}^{\infty + i\epsilon} + \int_{|k|/M - \delta + i\epsilon}^{\infty + i\epsilon} \right) \times \tilde{f}_{k}(\omega) e^{-y^{\sigma} \sqrt{\hat{k}^{2} - \omega^{2}}} d\omega \equiv l_{1} + l_{2} + l_{3} \quad (A5)$$

where  $\epsilon$  and  $\delta$  are infinitesimally small. Furthermore, we assume that

$$\left| \tilde{f}_k(\omega) \right| \le C \epsilon^{-D|\omega|} \tag{A6}$$

for  $|\omega| > \Omega_0$  where C and D are positive constants and  $\Omega_0$  is some large value.

Then, integrals  $I_1$ ,  $I_2$  and  $I_3$  can be estimated as follows. For  $I_1$ , we have

$$|I_{1}| \leq \frac{1}{2\pi} \int_{-\infty+i\epsilon}^{-|k|/M+\delta+i\epsilon} \left| \tilde{f}_{k}(\omega) e^{-M^{\alpha} \eta \sqrt{(k/M)^{2}-\omega^{2}}} e^{-i\omega t^{\alpha}} \right| d\omega$$

$$\leq \frac{1}{2\pi} \int_{-\infty+i\epsilon}^{-|k|/M+\delta+i\epsilon} \left| \tilde{f}_{k}(\omega) \right| e^{\epsilon t^{\alpha}} d\omega$$

$$\leq \frac{1}{2\pi} e^{\epsilon t^{\alpha}} \int_{-\infty+i\epsilon}^{-|k|/M+\delta+i\epsilon} e^{\epsilon t^{\alpha}} \int_{-\infty+i\epsilon}^{-|k|/M+\delta} e^{\epsilon t^{\alpha}} \int_{-\infty}^{-|k|/M+\delta} e^{\epsilon t^{\alpha}} \int_{-\infty}^{-|k|/M+\delta} e^{\epsilon t^{\alpha}} ds$$

$$\leq \frac{1}{2\pi} e^{\epsilon t^{\alpha}} \int_{-\infty}^{-|k|/M+\delta} e^{\epsilon t^{\alpha}} e^{-D(k/M+\delta)} \leq \frac{C}{2\pi D} e^{\epsilon t^{\alpha}} e^{-Dk/M}$$

$$= \frac{1}{2\pi} \frac{C}{D} e^{\epsilon t^{\alpha}} e^{-D(k/M+\delta)} \leq \frac{C}{2\pi D} e^{\epsilon t^{\alpha}} e^{-Dk/M}$$

$$(A7)$$

Similarly, it can be shown that

$$|I_3| < \frac{C}{2\pi D} e^{\epsilon t^{\alpha}} e^{-Dk/M} \tag{A8}$$

For  $I_2$ , we note that, since now  $|\omega| < |k|/M$ ,

$$\begin{split} M^{\alpha}\eta\sqrt{\frac{k^2}{M^2}-\omega^2} &= M^{\alpha-1}\eta|k|\sqrt{1-\left(\frac{M\omega}{k}\right)^2} \\ &= M^{\alpha-1}\eta|k|\left(1-\frac{1}{2}\left(\frac{M\omega}{k}\right)^2+\cdots\right) \\ &= M^{\alpha-1}\eta|k|-\frac{1}{2}M^{\alpha+1}\frac{\eta\omega^2}{|k|}+\cdots \end{split}$$

Thus, for the leading term as M = 0,

$$I_{2} = \frac{1}{2\pi} \int_{-|k|/M - \delta + i\epsilon}^{|k|/M - \delta + i\epsilon} \tilde{f}_{k}(\omega) e^{-M^{\alpha - 1}\eta|k|} e^{-i\omega t} d\omega$$

$$= \frac{1}{2\pi} e^{-M^{\alpha - 1}\eta|k|} \int_{-|k|/M + \delta + i\epsilon}^{|k|/M - \delta + i\epsilon} \tilde{f}_{k}(\omega) e^{-i\omega t} d\omega$$

$$= \frac{1}{2\pi} e^{-M^{\alpha - 1}\eta|k|} \left( \int_{-\infty + i\epsilon}^{\infty + i\epsilon} - \int_{-\infty + i\epsilon}^{-|k|/M + \delta + i\epsilon} - \int_{|k|/M - \delta + i\epsilon}^{\infty + i\epsilon} \right)$$

$$\times \tilde{f}_{k}(\omega) e^{-i\omega t} d\omega$$

It is easy to verify that the first integral is  $f_k(t^o)$  and the last two integrals are of order  $e^{-Dk/M}$ . Thus, to leading order,

$$I_2 = e^{-M^{\alpha - 1}\eta|k|} f_k(t^{\sigma}) \tag{A9}$$

By comparing (A7), (A8) and (A9), it is seen that  $I_1$  and  $I_3$  are exponentially smaller than  $I_2$ . Thus, we get the leading term of  $p^{\alpha}_{k}$  as

$$p^{o}_{k} \approx e^{-M^{\alpha-1}\eta|k|} f_{k}(t^{o})$$
 (A10)

# ACKNOWLEDGMENT

This work was supported by the National Aeronautics and Space Administration under NASA Contract NAS1-19480 while the authors were in residence at the Institute for Computer Applications in Science

and Engineering, NASA Langley Research Center, Hampton, VA 23681.

# REFERENCES

- M. Abramowitz and I. A. Stegun, Handbook of Mathematical Functions, Dover, New York, 1965.
- G. K. Batchelor, An Introduction to Fluid Mechanics (Cambridge University Press, 1967).
- D. G. Crighton, "Basic principles of aerodynamic noise generation", Prog. Aerospace Sci, 16, No. 1, 31-96, 1975.
- 4. S. C. Crow, "Aerodynamic sound emission as a singular perturbation problem", Stud. Appl. Math., 49 (1), 21-, 1970.
- M. S. Howe, "Contribution to the theory of aerodynamic sound, with application to excess jet noise and the theory of the flute", Journal of Fluid Mechanics, 71 (4), 625-673, 1975.
- T. Kambe, "Aerodynamic sound associated with vortex motions: observation and computation", Theoretical and Applied Mechanics, Bodher et al (editors), Elsevier, 1993.
- O. Knio, L. Collorec and D. Juve, "Numerical study of sound emission by 2D regular and chaotic vortex configurations", Journal of Computational Physics, 116, 226-246, 1995.
- J. Laufer, J. E. Ffowcs Williams and S. Childress, "Mechanism of noise generation in the turbulent boundary layer", AGARDograph 90,, 1964.
- A. Leonard, "Vortex methods for flow simulation", Journal of Computational Physics, 37, 289, 1980.
- M. J. Lighthill, "On sound generated aerodynamically, I. General theory", Proc. Roy. Soc. Lond., 211, 564-, 1952.
- 11. A. Michalke, "On the inviscid instability of the hyperbolic-tangent velocity profile," J. Fluid

- Mech. 19, 543, 1964,
- L. Morino and M. Gennaretti, "Boundary integral equation method for aerodynamics", Computational Nonlinear Mechanics in Aerospace Engineering, edited by S. N. Atluri, 279-320, 1992.
- Y. Nakamura, A. Leonard and P. Spalart, "Vortex simulation of an inviscid shear layer," AIAA Paper No. 82-0948, 1982.
- E.-A. Muller and F. Obermeier, "The spinning vortices as a source of sound", AGARD CP22, Paper 22, 1967.
- A. Powell, "Theory of vortex sound", J. Acoust. Soc. Am., 16, 177-195, 1964.
- E. Zauderer, Partial Differential Equations of Applied Mathematics, John Wiley & Sons, 1983.

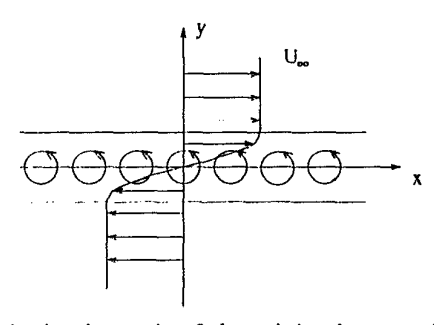


Figure 1. A schematic of the mixing layer and vortex blobs.

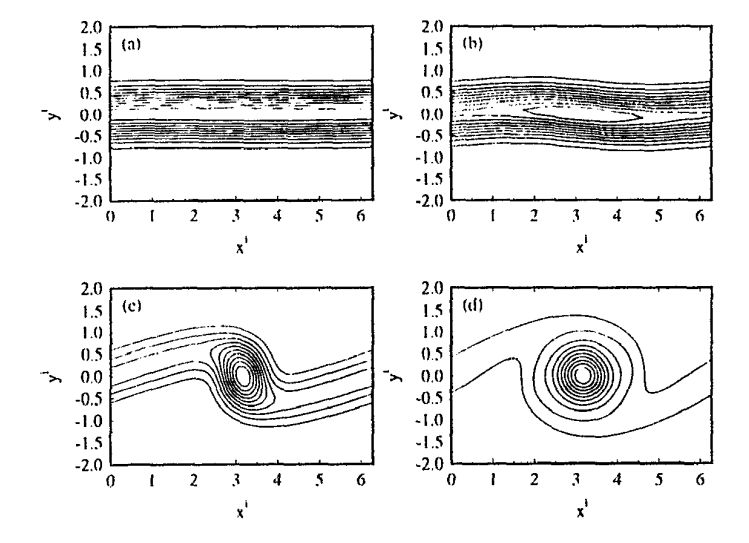


Figure 2. Contours of vorticity at selected time steps showing the growth of Kelvin-Helmholtz instability wave.

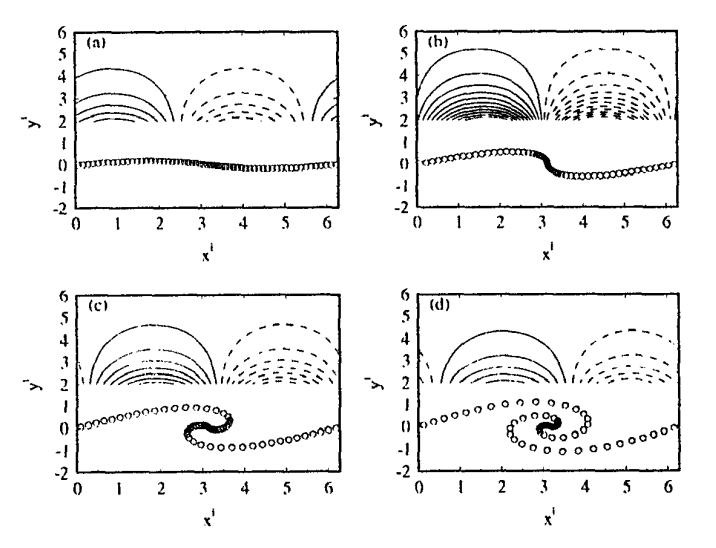


Figure 3. Vortex blob positions and the contours of the induced pressure field above the mixing layer at selected time steps.

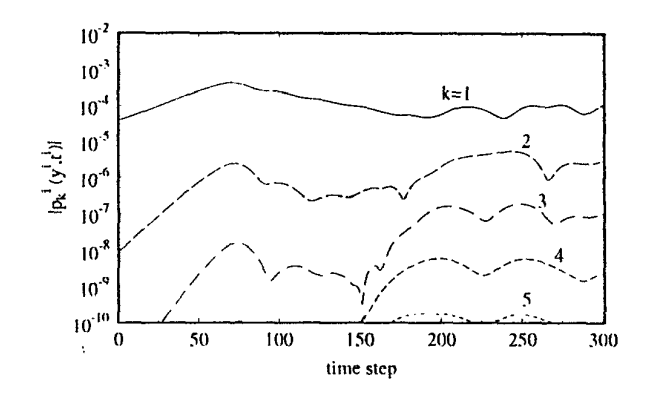


Figure 4. Amplitudes of the pressure as functions of time  $t^i$  for Fourier modes with k = 1, 2, 3, 4, 5.

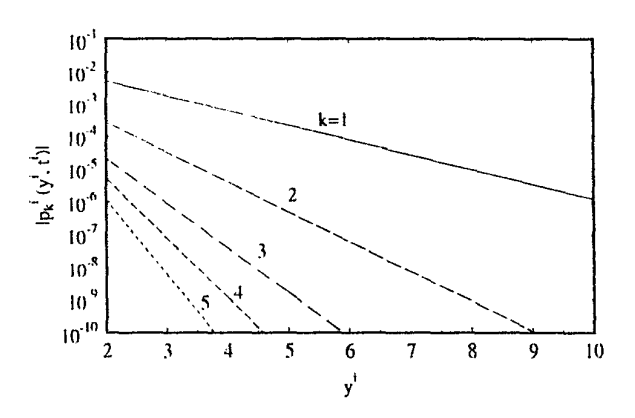
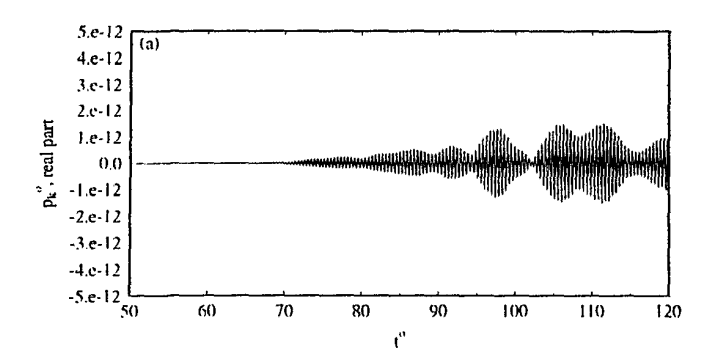


Figure 5. Amplitude of the pressure as a function of  $y^i$  for Fourier modes with k = 1, 2, 3, 4, 5.



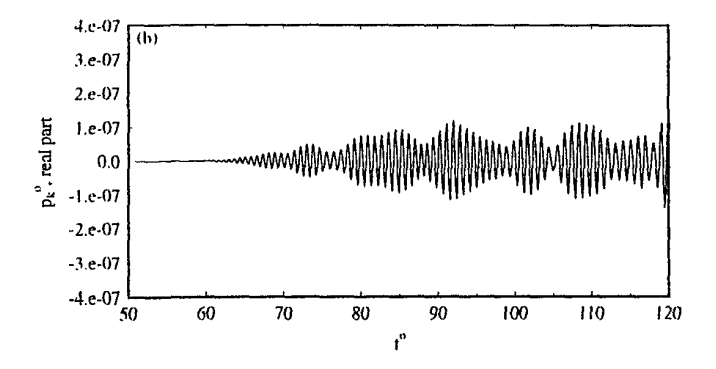


Figure 6. Amplitude of the acoustic pressure as a function of time  $t^o$  for k=1. (a) M=0.08, (b) M=0.16.

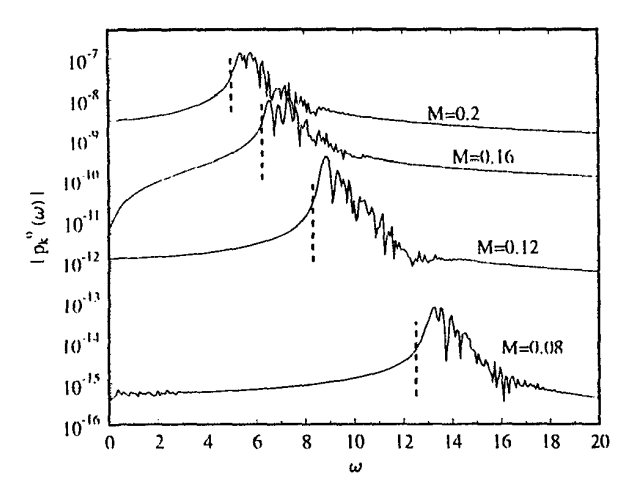


Figure 7. Spectrum of the acoustic pressure for k=1. The dashed lines indicate the sonic phase speed  $\omega=k/M$ .

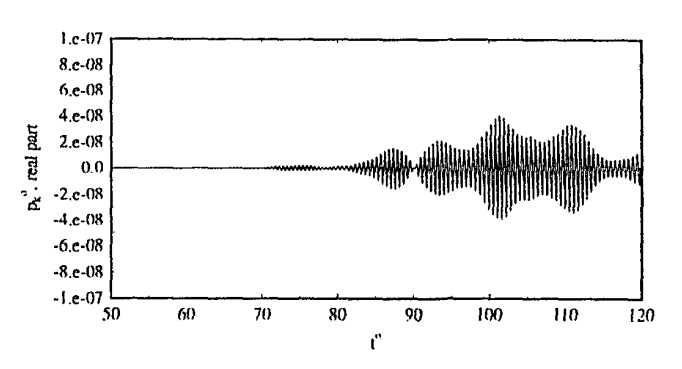


Figure 8. Acoustic pressure as a function of time  $t^{o}$  for k=2 and M=0.2.

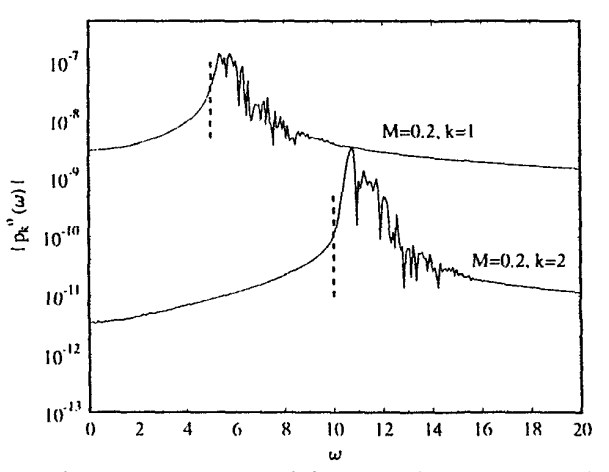


Figure 9. Spectrum of the acoustic pressure for k=1 and k=2 with M=0.2. Dash lines indicate the sonic phase speed  $\omega=k/M$ .